*Energy Equip. Sys. / Vol. 9/No. 2/June 2021/ 127-143*

ENERGY EQUIPSYS

Energy Equipment and Systems

http://energyequipsys.ut.ac.ir
www.energyequipsys.com

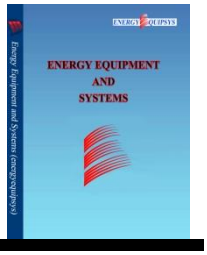


# Assessment and multi-objective optimization of an off-grid solar based energy system for a Conex

**Authors**

**Melika Sadat Taslimi** [a]
**Sajad Maleki Dastjerdi** [a]
**Shadi Bashiri Mousavi** [a]
**Pouria Ahmadi** [a*]
**Mehdi Ashjaee** [a]

[a] School of Mechanical Engineering, College of Engineering, University of Tehran, P.O. Box 11155-4563, Tehran, Iran

*Article history*:

Received : 11 February 2020
Accepted : 16 March 2020

**ABSTRACT**

*In this study, an off-grid PV system is optimized to supply a Conex electricity demand in the top ten earthquake-prone cities using mixed-integer linear programming techniques. The stand-alone photovoltaic system is designed by a photovoltaic array, a cooling/heating system, battery banks, an inverter, and a charge controller. For determining the optimum size and specifications of the system components such as PV panel, HVAC coefficient of performance, by considering two objectives of the study, a mixed-integer linear programming method is used. These conflicting objectives are the probability of lack of power and total cost of the system. The weighted factor method is utilized, and final optimized systems are achieved using MATLAB 2019b. Using the weighted factor method, several optimum solutions, in which the importance of objectives are different from each other, are obtained for each case concerning objectives. The suggested model is optimized for ten earthquake-prone cities globally, while it can be utilized for any location. The Pareto frontiers are presented to show the trade-offs between two objective functions. The average cost of off-grid PV system supplied electrical power is from about 1000$ for lima (subtropical desert climate) to 4000$ for Tokyo and Osaka (humid subtropical). Analysis of obtained results demonstrates that the system is suitable for all of the considered cities. It can supply the load demand of an off-grid Conex with a loss of power supply probability as low as 1%.*

**Keywords:** Off-Grid PV System; Multi-Objective Optimization; Mixed-Integer Linear Programming, Earthquake-Prone Cities.

## 1. Introduction

Environmental problems have been attracted attention recently. One of the crucial problems is global warming due to using fossil fuels for producing required energy. Besides, an increase in electricity demand imposes local energy potentials, renewable energy sources, which are efficient and feasible solutions[1]. A large number of renewable energy sources are available and can be used in different situations. Among available sources, a photovoltaic (PV) system is suitable for off-grid systems. Also, PV can be used in hybrid off-grid systems. Roughly about 1.4 billion people worldwide, living in rustic regions, do not have access to the electrical grid [2]. Therefore, off-grid PV systems are increasingly used in off-grid areas to supply electrical demands. Moreover, natural disasters, such as floods or earthquakes, destruct hundreds of houses worldwide, and temporary structures like Conex may be used for people who lose their homes. Electrical requirements of people during this time in which they are homeless must be provided. Thus, off-grid PV

* Corresponding author: Pouria Ahmadi
School of Mechanical Engineering, College of Engineering, University of Tehran, P.O. Box 11155-4563, Tehran, Iran
Email: Pahmadi@ut.ac.ir

systems can be utilized due to their cost efficiency, portability, and easy installation. Thus, Conex with suitable off-grid energy suppliers is useful for earthquake-prone districts in the world. For this off-grid Conex, PV systems must be sized and selected to supply all electricity requirements of the Conex. Also, in terms of economic aspects, these PV systems must be worked in their optimum situations to be cost-effective and must not be oversized/undersized. One of the most crucial parts of designing off-grid PV systems is the sizing of PV arrays and storage capacity. Electricity storages are required due to the lack of required sun irradiation during nights or cloudy days. For achieving related and required information, a considerable number of related literature are summarized as below.

First of all, based on the reviewed literature, different methods can be used for designing and sizing PV systems. These models include numerical and analytical methods [3]. Apart from these models, another one is heuristic [4]. Intuitive methods can result in oversizing or under-sizing. It happens due to the designing procedure of this method in which the worst month in a year in terms of solar energy or monthly/yearly average is considered a input of the method. Analytical methods, as another one, have equations that state PV sizes as a function of reliability. These models have a lower computation cost, and their equations are location-dependent and challenging for developing [5, 6]. Another solution is using hourly/daily radiation and energy requirement to balance the system, and this solution is a numerical method. All of the energy productions and requirements in every time step are considered, resulting in optimal sizing of the PV systems [3, 7, 8]. PV system optimizations using heuristic methods have been done in several studies [9-11]. But due to the procedure of these methods, they cannot find out optimal system necessarily [12]. PV systems are usually utilized. in regions that have suitable solar irradiation. Three studies evaluated the optimization of off-grid PV systems in Malaysia. In these studies, the used method was iterative, which resulted in an optimum PV system. They showed that these optimum PV systems can supply all of the required electricity demand of off-grid systems [13-15]. Ayop et al. evaluated different methods for sizing standalone PV systems. Evaluated methods were iterative ones. The reliability of the off-grid PV system was boosted using the reliability improvement method. They showed that the life cycle cost (LCC) method is more accurate in predicting the overall costs of the system in its lifespan [16]. Andam, et al. studied optimization of off-grid PV system located in rural area of Morocco. They considered lack of energy during a year and then optimized system in order to protect system from oversizing or under-sizing. They showed that this optimal PV system can supply energy requirement of a house with 5 occupants [17]. Load fluctuation can have a significant impact on the performance of an off-grid PV system. In this way, a slight increase in the load demand can cause a power shortage in a system [18]. Khalil and Asheibi optimized a standalone PV system using the grey wolf method, and the cost of the system during its lifetime was their objective. They showed that using this method optimal system can be achieved [19]. Semaoui et al. proposed a model for optimizing off-grid PV systems by considering load management. They used MATLAB Simulink for modeling PV system components. This model has two optimization criteria. One of them is loss of power supply probability, and another one is the cost of the system. They used this model for a house in Algeria. They showed that this load management results in cost reduction and system reliability [20]. Behzadi and Roshandel optimized the hybrid energy system for educational buildings with PV, wind turbines, batteries, and diesel generators. Their objectives were cost of fuel and battery wear cost. They showed that this optimization improved energy production of the system up to 18.7%. Also, they showed that season changes affect operation of the system [21].

Based on the usage and importance of off-grid Conex in earthquake-prone regions in the world in this research study, an optimization model based on Mixed-Integer Linear Programming (MILP) for the adoption of a stand-alone PV system in the remote area in the top ten earthquake-prone cities in the in the world is proposed.. The life span of the system has been considered 20 years. The model is utilized in ten cities, including Tokyo, Jakarta,

Manila, Los Angles, Quito, Osaka, San Francisco, Lima, Tehran, Istanbul. This system consists of PV panels, a cooling/heating device, a battery, an inverter, and a charge controller. This system has been optimized to supply the electricity requirement of off-grid Conex. PV panels collect solar radiation and produce electricity which can be stored in the battery or used in Conex. The optimization procedure minimizes the total cost and LPSP of the system and specifies the area of photovoltaic panels, HVAC system specifications, and the size of the battery. It happens concerning hourly load demand and solar radiation, which are achieved using TRNSYS software. Then, they have been used in MATLAB for determining optimal solution [22, 23]. To the best of our knowledge and based on the reviewed literature, there is no study on off-grid PV Conex in the mentioned earthquake-prone cities. Sub-objectives and novelties of this study can be summarized as below:

- Modeling and predicting the performance of off-grid Conex in top ten earthquake-prone cities in the world.
- Optimizing the PV system according to hourly input data using multi-objective optimization.
- Optimizing specifications of PV panels and their area.
- Proposing an off-grid PV system for practical aims.
- Considering available options in the market as decision variables.

## 2. Modeling

For designing an off-grid Conex in this study, PV panels must supply the electricity consumption of Conex. For this, a standard container produced by GCC company has been considered as Conex. Then required PV panels with optimum slope angle have been attached to the Conex. In Fig. 1, a schematic of designed off-grid Conex in this study can be seen. Specifications of the selected Conex can be seen in Table 1. Electrical equipment of this Conex is typical for the residential building including, lightening (20W), a refrigerator (100W), and two Laptops (160W). The working time of the laptop has been considered from 8 a.m. to 4 p.m. (office hours). Another device is a cooling/heating system [24].

**Fig. 1.** Proposed Conex with its off-grid PV system

**Table 1.** Selected Conex specifications

| **Dimensions [mm$^3$]** | **2.5∗2.7∗6** |
|---|---|
| Walls | 4cm thick, Polyurethane |
| Roof | 5cm thick, Polyurethane |
| Window | 2.285 length, Double pane Argon gas |

### 2.1. Locations

As explained earlier, the proposed photovoltaic system is intended to be utilized in earthquake-prone regions as a temporary residence. Therefore, the ten most earthquake-prone cities worldwide are considered locations of the proposed system: Tokyo, Jakarta, Manila, Los Angeles, Quito, Osaka, San Francisco, Lima, Tehran, Istanbul. These are the cities experts believe are the most likely to experience a significant earthquake [25]. The properties and climate types of the cities are presented in Table 2. Based on the population of the earthquake-prone cities, a temporary residence is significantly beneficial.

### 2.2. System components and properties

First of all, for PV system design, the performance of different subsystems must be evaluated based on the related input data. Therefore, in this part, used mathematical and technical models are described. In this system, PV panels produce electricity. Produced electricity will be sent to the battery or Conex. The charge controller determines the place in which electricity will be sent. Apart from this decision-making, this device will protect the battery from overcharging and deep discharging and provide user errors. Battery saves extra produced power which is used on nights and cloudy days for supplying energy requirement. Produced electricity by PV panels is DC, but building devices need AC. Therefore, in this system inverter is used to convert DC to AC. During system sizing, designers have to forecast electricity consumption and generation so that the proposed system can overcome the sizing requirement (i.e., energy demand). For achieving this aim, related data, including ambient temperature, HVAC loads of Conex, and hourly solar radiation, are needed. Hourly or daily solar radiation and ambient temperature data are rarely available or may not be long enough to permit long-term performance analysis. Therefore, Klein and Beckman [29] proved that synthetic data could be utilized where no actual data exist. Meteonorm is one of the best sources of solar radiation and ambient temperature data widely used in the literature for solar system performance assessment [30]. Employing the input/output technical model for subsystems, the power generation at each time interval, electrical requirement, the accumulated energy at the battery bank, and the unmet electrical demand is calculated each time step in an hour. In this study, for simplification, performance simulation of charge controller and inverter is ignored.

#### 2.2.1. Heating and cooling loads/Estimation of load demand

One of the electricity consumption parts of the Conex, which must be supplied, is the required energy of the heating/cooling device. This load is calculated hourly using TRNSYS software [31]. The simulated system in TRNSYS can be seen in Fig. 2.
Employed components in TRNSYS simulation are gathered in Table 3.

**Table 2.**Selected cities information

| City | Country | Area ($km^2$) [26] | Population [27] | Climate type [28] |
|---|---|---|---|---|
| Tokyo | Japan | 2.194 | 37,435,191 | Humid subtropical |
| Jakarta | Indonesia | 661.5 | 10,915,364 | Tropical monsoon |
| Manila | Philippines | 42.88 | 14,158,573 | Tropical wet and dry |
| Los Angeles | United States | 1302 | 3,983,540 | Mediterranean |
| Quito | Ecuador | 372.4 | 1,900,571 | Subtropical highland |
| Osaka | Japan | 223 | 19,222,665 | Humid subtropical |
| San Francisco | United States | 121.4 | 883,255 | Warm-summer Mediterranean |
| Lima | Peru | 2672 | 10,882,757 | Subtropical desert |
| Tehran | Iran | 730 | 9,259,009 | Mediterranean |
| Istanbul | Turkey | 5343 | 15,415,197 | Mediterranean |

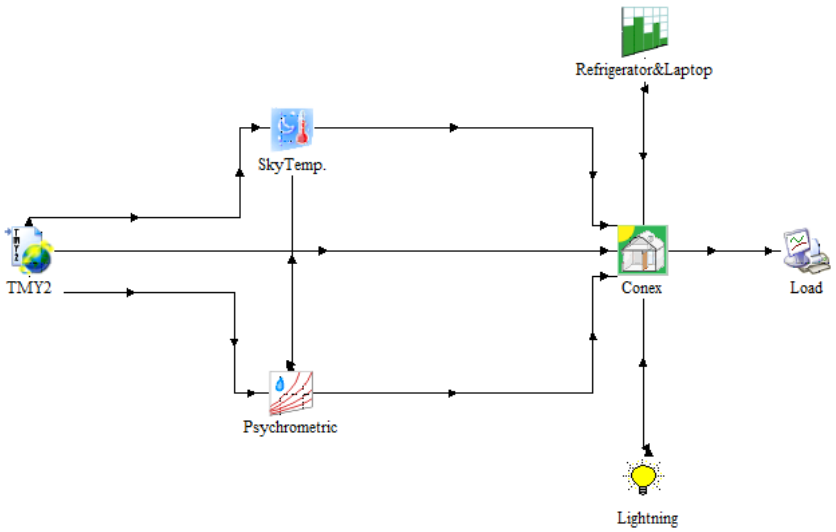


**Fig. 2.** Schematic simulation model in TRNSYS

**Table 3.**Employed components in TRNSYS

| Num. | Component name | Input | Output |
|---|---|---|---|
| 1 | Data reader and radiation processor | tm2 file | Temperature, irradiance, wind speed, etc. |
| 2 | Psychrometrics | Dry bulb temperature, humidity | Psychrometrics Data |
| 3 | Effective sky temperature for long-wave radiation exchange | Radiation data | Effective sky temperature |
| 4 | Multi-zone building | Building and climate data | HVAC loads, Inside temperature, etc. |
| 5 | Time-dependent forcing function. | - | Time-dependent schedule |
| 6 | Online graphical plotter | The output of other components | plot |

Polyurethane is the material of the roof and walls of the Conex. The thermal conductivity of polyurethane is about 0.022 W/mK. The window is mounted on the south wall, and it is a double pane argon gas window. The setpoint temperature for cooling and heating is 25° C and 22° C.

Based on the calculated HVAC loads of Conex and because PV panels produce electricity, a split HVAC system has been considered. The coefficient of performance of this heating/cooling system is about 3.6 and will maintain the Conex inside temperature at the desired level. The following figures show the measured monthly electrical demand profile, which the proposed PV system should provide for each city. The electrical requirement of the Conex includes lighting, laptop, refrigerator, and HVAC system.

Variation of Conex loads and solar radiation for considered cities in a year can be seen in Fig. 3 to Fig. 7. Total load includes heating and cooling load plus appliance load. The most earthquake-prone cities in South America are Quito and Lima. Variation of their loads and radiation can be seen in Fig. 3. As shown in Fig. 3 in Quito, solar radiation increases from the first of the year to its maximum at the 2$^{nd}$ month, then decreases continuously to its lowest in June and then increases to its maximum in October and reduces to December. A total load of this city is roughly equal to solar radiation of 1 m$^2$ in January and November. Therefore, if the PV panel area is equal to one square meter, load demand cannot be supplied using PV panels in these months. In lima, total load decrease from the first of the year to October and then boosts to the end of the year. In both cities, most of the

load is for appliances. The maximum load of lima and Quito are approximately equal, but unlike Lima, Quito load is roughly constant during a year. Solar radiation in lima is much higher than in Quito, and its variation pattern is the same as in Quito. Therefore, unlike Quito, load demand in lima can be supplied easily in all months of the year.

In the USA (Fig. 4), the most earthquake-prone cities have the same radiation variation pattern during a year. Solar radiation rises from January to its maximum in July then decreases to its yearly lowest in December. Likewise, in terms of total load, again, the same pattern can be seen. Total load from its yearly maximum in January falls to its yearly lowest in September and June for San Francisco and Los Angles. After their yearly lowest, this load boosts to its yearly maximum. The yearly lowest solar radiation of San Francisco is lower than Los Angles, but its yearly highest radiation is higher than Los Angles. Hence solar radiation of San Francisco has more intense changes during a year. Total load of Los Angles in all months of the year is lower than solar radiation per square meter, and the lowest difference is in January, in which they are close together. But in San Francisco, the total load is higher than solar radiation of 1 $m^2$ in January, February, November, and December. Hence, the PV panel area for this city must be higher than 1 $m^2$ to supply the load demand.

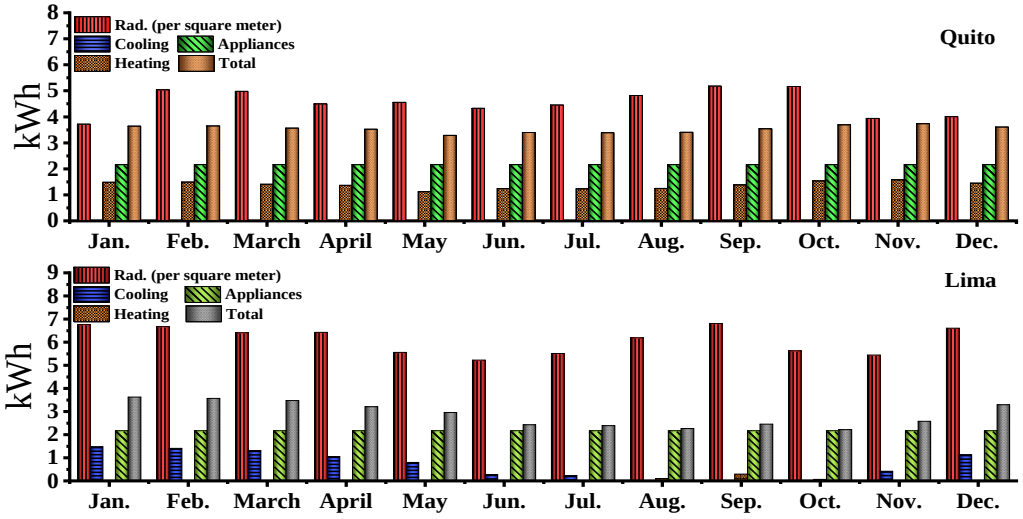


**Fig. 3**. South America (loads and radiation)

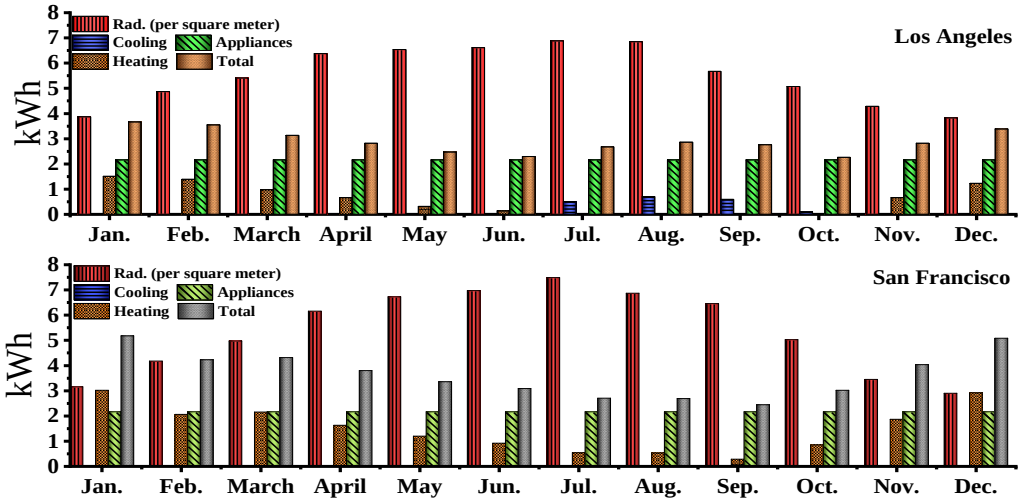


**Fig. 4.** USA (loads and radiation)

In east Asia, for Manila and Jakarta similar solar radiation pattern can be seen in a year (Fig. 5). The yearly highest in Jakarta happens in September, but for Manila, it is in April. The yearly lowest happens in January and August for Jakarta and Manila, respectively. The total load in Jakarta is roughly constant during a year. Unlike Jakarta,in Manila total load varies during a year and is close to solar radiation in August. Most of the total load in Manila is cooling load due to its climate and ambient temperature. In Jakarta, total load demand is higher than solar radiation of one square meter in January and April. Therefore, the PV area must be higher than one square meter. Due to these cities' high ambient temperature and climate, heating load is not required during a year.

In west Asia, solar radiation in Istanbul from January to April increases and reaches its yearly highest, after that decreases continuously to August and after that boosts and is roughly constant during next months, Fig. 6. In Tehran, solar radiation rises from the first of the year to its yearly maximum in August and then falls to its yearly lowest in December. Due to its environment, temperature, and climate, Istanbul does not need heating for a year (Fig. 6). But Tehran needs heating in 7 cold months of a year. This is because the total load in Istanbul in all months of the year is lower than solar radiation of 1 $m^2$. But in Tehran, in January and December, solar radiation of one square meter is lower than total load demand.

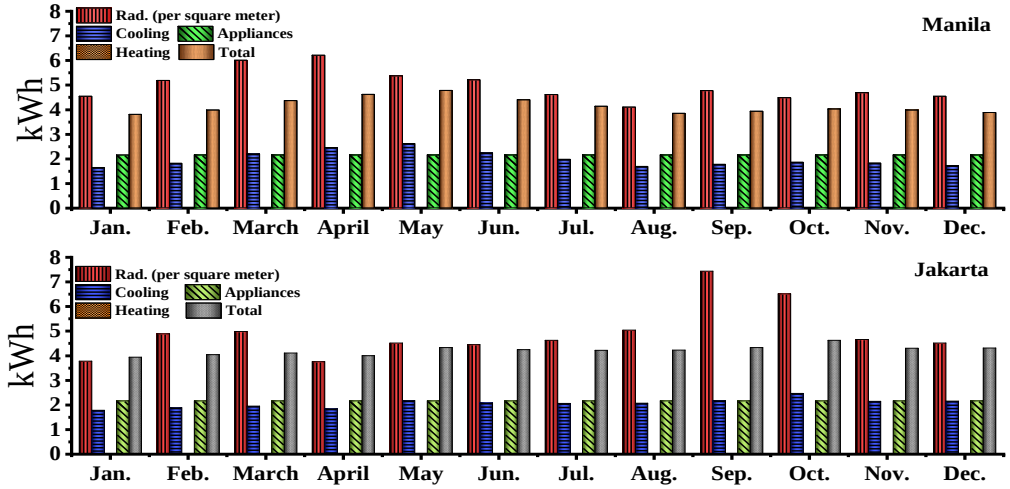


**Fig. 5.** East Asia (loads and radiation)

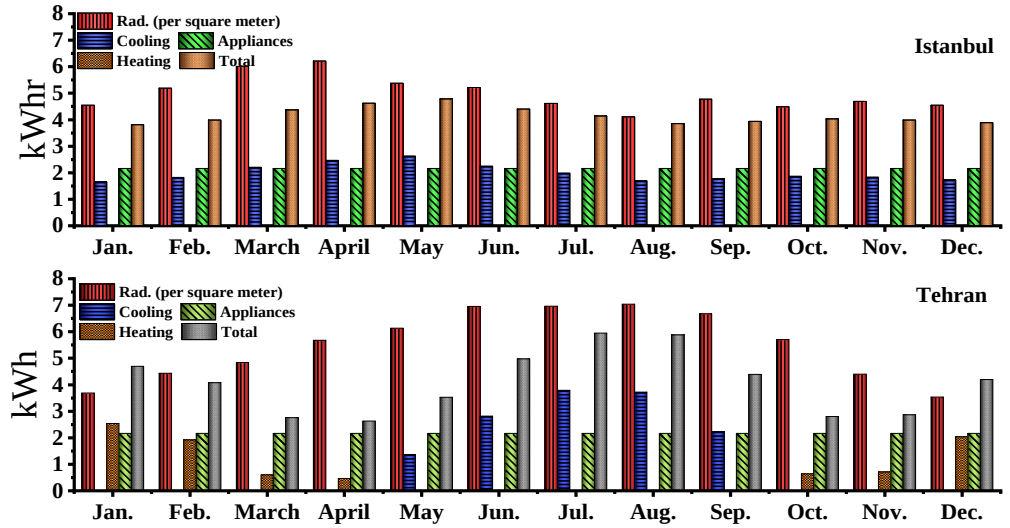


**Fig. 6.** West Asia (loads and radiation)

In Japan (Fig. 7), both heating and cooling are needed during a year. Solar radiation for 1 $m^2$ is lower than previously studied cities, and Tokyo is roughly constant during a year. In Osaka, solar radiation is increasing from the first of the year to May and likely from June to August. Then it is falling from August to December. The total load has the same variation pattern in both cities, Fig. 7. It drops from January to May, and increases from May to August and again falls to October and rises to the end of the year. Both heating and cooling for Tokyo are much bigger than for Osaka. Solar radiation of 1 square meter in Tokyo is lower than the total load in a year except in October and May. In Osaka, solar radiation per square meter is lower than the total load in the first three months of the year and the last second months. Therefore, in both cities, the PV panel area must be bigger than 1$m^2$.

### 2.2.2. Photovoltaic Array

Three parameters are needed for analyzing the performance of the PV panel. They are solar irradiance, PV characteristics, and ambient temperature. In addition, the produced power of PV panels must meet total daily load demand, plus extra energy to compensate system losses. The governing equation for a PV panel, according to the energy side that is widely investigated among researchers, is [32]:

$$P_{PV}(t) = \eta_{PV}\eta_{PV,T}A_{PV}G(t) \quad (1)$$

$$\eta_{PV,T}(T_c) = \eta_{PV,T}(25℃)[1 + \alpha(\eta_T)(T_c - 25)] \quad (2)$$

In these equations, the output power is $P_{PV}(t)$. Panel efficiency is $\eta_{PV}$. Total solar radiation on the surface and total area of the panel is $G(t)$ and $A_{PV}$, respectively. Output power and total solar radiation are time-dependent parameters. Due to the economic aspects and available area on the roof of Conex, crystalline silicon photovoltaic panel is selected. This panel has a power output of 100-300 W. More information about this panel is provided in the multi-objective optimization part.

### 2.2.3. Storage System

Energy storage is an undeniable part of such an off-grid PV system. It happens due to fluctuating nature of renewable energy resources such as solar radiation. Also, another reason is the lack of solar radiation on cloudy days and nights. For this purpose, several types of energy storage can be used, such as compressed air, pumping water. But due to the importance of cost and space requirement of energy storage systems, a sealed-acid battery is preferred for this off-grid PV system [33-35]. Plenty number of parameters are considered in the battery selection procedure. Some of them are availability, proper size, matching with other equipment, and mobility.

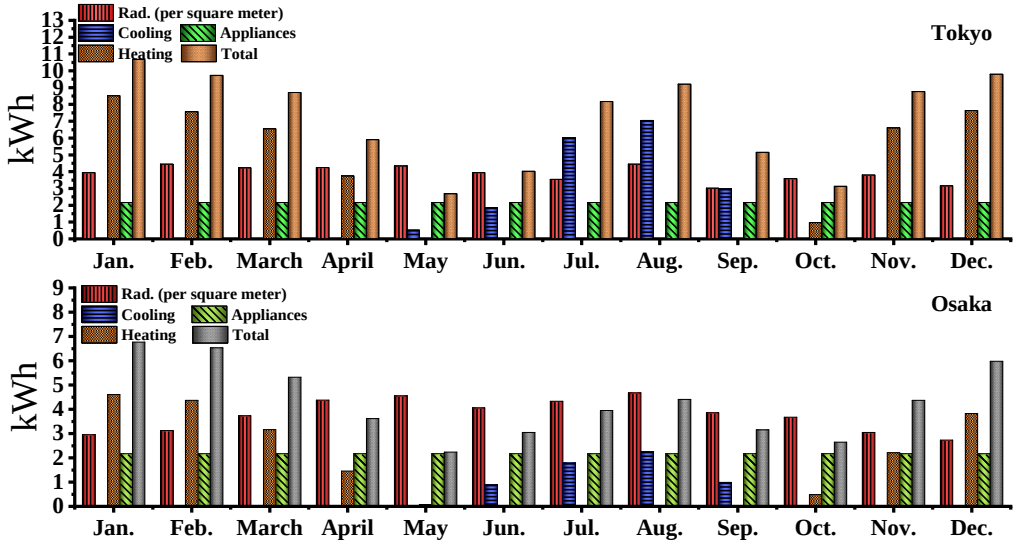


**Fig. 7.** Japan (loads and radiation)

Two crucial and primary parameters in battery operation are state of energy (SOE) and depth of discharge (DOD). DOD is an important parameter that affects battery lifetime. It determines the allowable discharge rate of battery for a longer lifespan; therefore, maximum DOD is assumed 80% in the sizing process [36]. SOE is the battery energy level [37]. The energy level of batteries can be computed using Eq.(3) [21].

$$SOE(\mathrm{t}+1) = \begin{cases} (1-\tau)\mathrm{SOE}(\mathrm{t}) + \eta_{\mathrm{ch}}\mathrm{P}_{\mathrm{ch}}(\mathrm{t}) \\ (1-\tau)\mathrm{SOE}(\mathrm{t}) - \dfrac{\mathrm{P}_{\mathrm{dis}}(\mathrm{t})}{\eta_{\mathrm{dis}}} \end{cases} \quad (3)$$

In this equation, SOE(t) and SOE(t+1) are the energy state of the batteries at the time of t and t+1, respectively. Battery charging and discharging efficiencies are $\eta_{ch}$ and $\eta_{dis}$, respectively. Also, $\tau$ is the self-discharge rate. As mentioned, for improving battery lifetime, battery energy cannot be lower than $SOE_{min}$ and higher than $SOE_{max}$, therefore excess produced energy will be lost. In this study, batteries are reachable solar batteries produced by CSBattery. The nominal voltage of this battery is 12 V, and its capacity is about 100 Ah to 200 Ah. In this study, unlike some studies, in which they determine the size of the battery in a way that can supply power consumption of the system for two autonomous days, for avoiding battery oversizing, battery capacity is considered one of the discission variables.

#### 2.2.4. Charge controller and Invertor

A charge controller is a device that manages energy flow in the solar system as a central point for loads, PV array, and battery bank. It also manages energy flows into the battery so that the battery will be provided with optimum charges to ensure subsystems (especially lamps and the battery bank) protected from deep discharges, overcharging, and fluctuation at voltage level [38]. There are two types of charge controllers commonly used for stand-alone photovoltaic purposes, pulse width modulation (PWM) and maximum power point tracking (MPPT). MPPT results in better charging efficiency of up to 30%, which causes better output for PV panels and has a short payback period [38]. In this study, due to the type of selected battery, the MPPT charge controller, ET4415BND, is selected as a suitable charge controller for this type of battery. As mentioned before inverter must supply AC power for Conex equipment from PV panels or batteries DC power. These devices do not have 100% efficiency. Therefore, some part of the produced power will be wasted. In this study, mathematical equation for modeling performance of charge controller and inverter is ignored in the optimization process.

### 2.3. Multi-Objective Optimization

To determine the best sizing and system configuration according to the decision variables, many objective functions can be considered. Most of them are associated with the reliability and cost of the system. In this research, the system's LPSP and cost are considered two objective functions of the optimization procedure. Based on these objective functions and using multi-objective optimization, decision variables are determined.

#### 2.3.1. Decision Variables and Objective Functions

As mentioned before, the objective functions of this study are LPSP and system cost. These objectives are conflicting terms. In other words, the system will be enlarged to achieve the first one, and likewise, system cost will be higher. Likely, second objective achievement results in a minor system and higher LPSP. The cost in this study includes the cost of PV panels, HVAC systems, and batteries. Battery cost includes initial and replacement costs. The system lifetime is considered 20 years, like PV panels lifespan. But batteries are usable for about five years [39]. Therefore, in the system, lifetime, batteries will be replaced four times. The cost is calculated using Eqs. (4) and (5).

$$C_{total} = C_{PV} + C_{Batteries,25year} + C_{cooling/heating\ system} \quad (4)$$

$$C_{Batteries,25year} = cost_{Batteries} \sum_{i=5,10,15} \frac{(i+1)^n - 1}{i(i+1)^n} \quad (5)$$

The load demand is satisfied with the energy produced by the PV panel or from the battery bank energy if PV panel power is not accessible. The system's reliability in terms of supplying load demand may be calculated using Eq. (6) [40].

$$LPSP = \frac{\sum_{t=1}^{8760} LPS(t)}{\sum_{t=1}^{8760} D(t)} \times 100 \quad (6)$$

One of the typical methods for the optimization process is the weighted function. In this method, all objectives are combined, and one single objective will be generated [41]. However, units of objectives are not equal. For solving this problem, cost terms are normalized using the highest possible system cost [42]. For implementing constraints, linear equations are used in this study for considering physical limitation. Due to the variable types, which are integer and continuous, mixed-integer linear programming (MILP) is used (Eq. (7) to (13)).

$$Min\ Z = \omega_1\ C_{total} + \omega_2 LSPS \quad (7)$$

$S.t.$

$$P_{ch}(t) - P_{dis}(t) - LSPS(t) \leq P_{PV}(t) - D(t) - \left(\frac{L(t)}{COP}\right) \quad (8)$$

$$P_{ch}(t) \leq \delta(t).M \quad (9)$$

$$P_{dis}(t) \leq (1 - \delta(t)).M \quad (10)$$

$$SOE(t) = SOE(t-1)(1-\tau) + \eta_{ch} P_{ch} - \frac{P_{dis}}{\eta_{dis}} \quad (11)$$

$$SOE(t) \leq 0.8 \times SOE_{max} \quad (12)$$

$$SOE(t) \geq 0.2 \times SOE_{min} \quad (13)$$

The balance of energy requirement and supply is evaluated in the first three equations. In these equations, the constant relaxation parameter is M and is much higher than other parameters. $\delta$ represents the binary variable which is 0 or 1. Accumulation of electrical loads except heating and cooling denotes D(t). Heating and cooling load represent with L(t). The HVAC coefficient of performance is COP. Equations 11 to 13 deal with battery SOE and its limitation. Decision variables are PV panel, HVAC system, and size of the battery. All decision variables are integer but battery size and HVAC selection. The cost and specifications of these parameters can be seen in the following tables. Prices were updated in May 2020. Calculations and optimizations are performed using MATLAB 2019b.

For PV panels, three models are considered, as can be seen in Table 4. All of them are crystalline silicon panels and suitable for off-grid electrification and roof installation. The nominal voltage of all of them is 12V.

As mentioned before, rechargeable batteries are selected. The capacity of them is between 100Ah and 200Ah. The average cost of them is about 0.812 $/Wh. The lower and upper bounds of the battery size are 1200Whr and 24000Whr. For the HVAC system, two split cooling/heating systems produced by LG company are considered, which can be seen in Table 5.

**Table 4.**PV panel choices

| Num. | Manufacture | Efficiency [%] | Price [$/W] |
|---|---|---|---|
| 1 | Haitai | 20.86 | 0.21 |
| 2 | Hancarve solar | 22 | 0.22 |
| 3 | PW | 18 | 0.14 |

**Table 5.** Split choices

| Num. | Model | Cooling COP | Heating COP | Price [$] |
|---|---|---|---|---|
| 1 | NF098ST1 | 3.68 | 3.93 | 625 |
| 2 | NT097SK1 | 3.21 | 3.62 | 440 |

## 3. Results and Discussion

The optimization process, utilizing mixed-integer linear programming, is done by MATLAB 2019b, resulting in optimal solutions for each earthquake-prone region. The optimal solutions are presented as Pareto frontiers for each city, demonstrating the trade-off between the total cost and the system reliability (LPSP). The Pareto frontiers of the ten cities are presented in Fig. 8 to Fig. 12, grouped concerning their location. Total cost is in dollars, and LPSP is exhibited in percentage. Notably, the presented cost in this part is the capital cost for having more tangible results. Due to the evident trade-off between the cost and LPSP in Fig. 8 - Fig. 12, there is plenty of optimum solutions for all cities in a considerable range of cost and reliability. The best option is selected concerning the application and suitable LPSP as well as the budget limit. As can be inferred from Fig. 8 to Fig. 12, optimum solutions for cities with higher radiation amplitude and lower load demand enjoy lower system cost. In the cooling and heating system selection, the first option of the split air conditioner with higher COP and higher cost is chosen in almost every optimum solution, demonstrating that the first option is more cost-efficient than the second one.

As two Japanese earthquake-prone cities in this study, Pareto frontiers of Tokyo and Osaka are presented in Fig. 8. Since there is significant load demand in both Tokyo and Osaka, the cost range in these two cities is far greater than in other regions, except for Istanbul. The optimum PV panel sizes in Tokyo and Osaka are between 3 to 10 kW, demonstrating the high demand and, more importantly, low radiation in these two cities. However, optimum options with LPSP lower than 1% have a lower cost in Tokyo than in Osaka due to the higher radiation amplitude in this city. The battery storage is calculated up to 8 kWh and 10 kWh for Tokyo and Osaka, respectively, the largest battery size of all options, except for Istanbul. Due to the low radiation amplitude of these two cities and their high heating and cooling loads during the year, more insulated Conex and other power suppliers such as a diesel engine or wind turbine are beneficial.

Pareto frontiers of two Southeast Asian cities, Manila and Jakarta, are illustrated in Fig. 9. The optimum solutions of the cities Manila and Jakarta have roughly the lowest cost due to high solar radiation and lower load demand in these cities. Therefore, as the two top earthquake-prone cities in danger, Manila and Jakarta can benefit from this stand-alone photovoltaic system for a temporary residential Conex. The PV panel size varies from 2.5 to 5 kWh in Manila optimum solutions and 2 to 5 kWh in Jakarta optimum solutions. Additionally, the battery size is selected up to 1.5 kWh, which is very practical since the system is less reliant on the storage system. As storage systems require replacement and also a considerable amount of energy is damped during charging and discharging the storage system, direct consumption is much better than employing large storage systems.

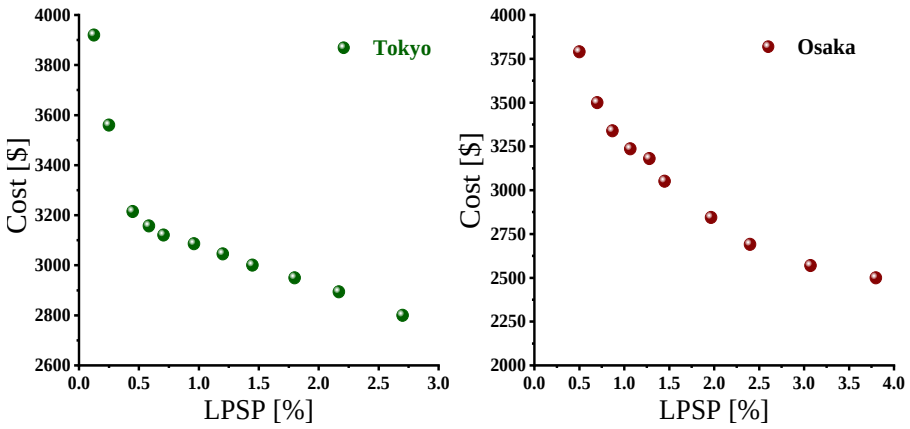


**Fig. 8.** Pareto frontiers for Tokyo and Osaka

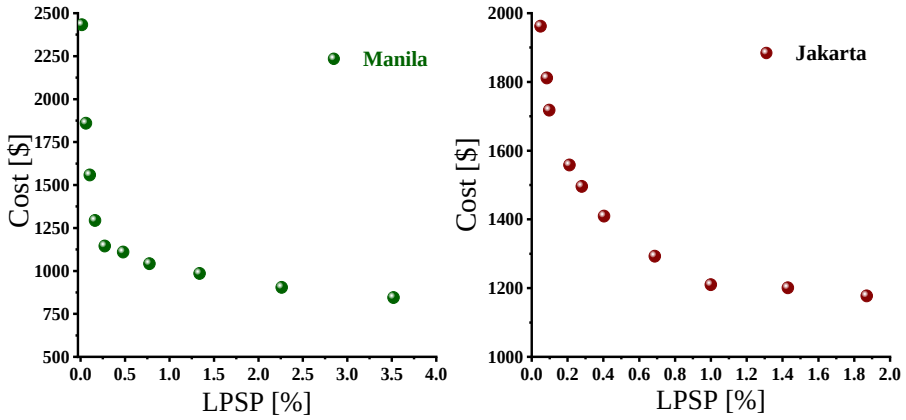


**Fig. 9.** Pareto frontiers for Manila and Jakarta

Pareto frontiers of two American earthquake-prone cities in California state, Los Angeles and San Francisco are displayed in Fig. 10. There is high radiation in both Los Angeles and San Francisco; however, higher load demand in San Francisco (mostly heating load) results in a more expensive optimum solution than in Los Angeles. Additionally, the lower cost of the optimum systems in Los Angeles is due to the higher radiation amplitude in this city. The PV panel size of the optimum options is between 1.8 to 5 kWh for Los Angeles and 2.5 to 9 kWh for San Francisco, as a result of their difference in load demand and radiation extent. The battery size for these cities is computed up to 5 and 7 kWh for Los Angeles and San Francisco, respectively. Despite the high load of the cities, especially San Francisco, a stand-alone photovoltaic system is a beneficial option for temporary residence due to the ample solar radiation in the cities.

Pareto frontiers of Quito and Lima, two earthquake-prone cities in South America, are depicted in Fig. 11. There is a significant amount of irradiation in both cities, resulting in the low cost of the photovoltaic system. Quito, having higher load demand, has a higher cost range, however. The LPSP span in these two cities is similar to that of Jakarta and Manila, and the system has suitable reliability. However, Lima has the lowest cost of all regions regarding its high solar radiation and low required load. The optimum photovoltaic panel size varies between 1.3 to 2 kWh for Lima and between 2.5 to 9 kWh for Quito. In addition, the battery storage is up to 2.5 kWh for Lima and up to 4 kWh for Quito in optimum results.

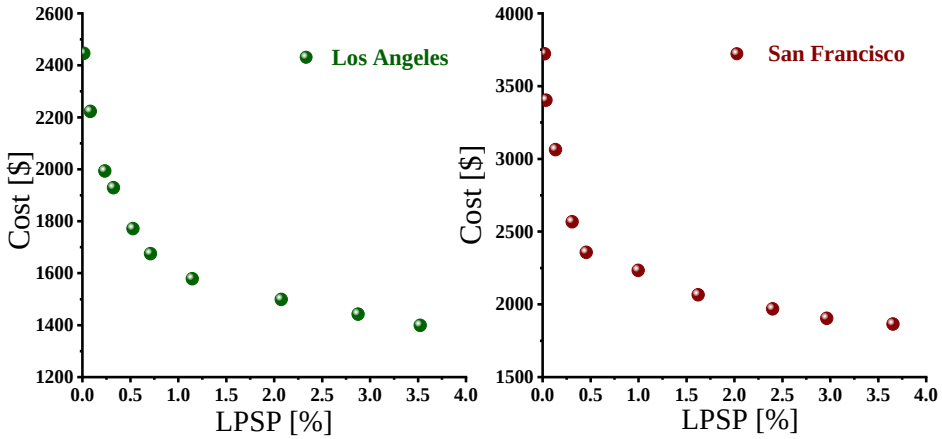


**Fig. 10.** Pareto frontiers for Los Angeles and San Francisco

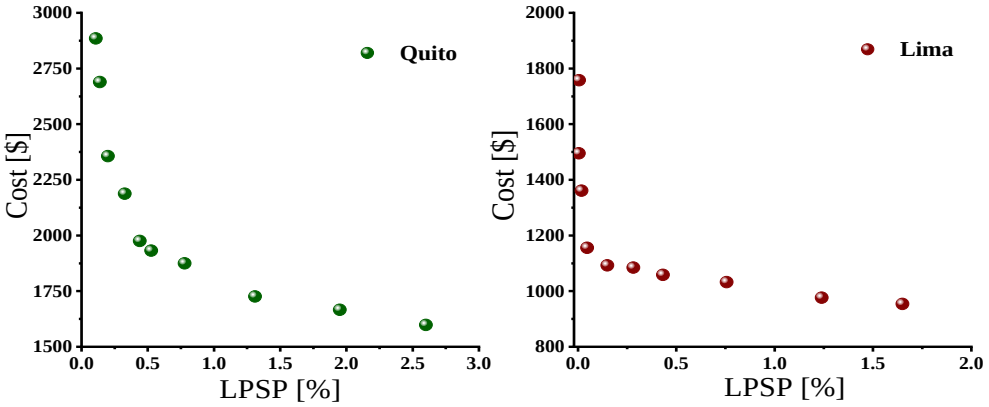


**Fig. 11.** Pareto frontiers for Quito and Lima

Pareto frontiers of Istanbul and Tehran, two earthquake-prone cities in West Asia, are presented in Fig. 12. Although there is a considerable amount of radiation in both cities, the high load demand of the cities results in the high cost of the optimum system. The cost range in Istanbul is roughly similar to that of Tokyo and Osaka. The PV panel size is from 2.5 to 9 kW in Tehran and from 2.5 to 10 kW in Istanbul due to their high required load. Also, the battery size increases up to 7 kWh in Tehran and up to 10 kWh in Istanbul. Therefore, a backup energy system and more insulated Conex are beneficial in these two cities, as well as Tokyo and Osaka. In order to comprehensive analysis of the system performance, some functioning variables are discussed. As the city with the biggest optimum results of all, Tokyo is considered, and one of the optimum solutions of this city (the one with equal weight factors of objective functions) is investigated. The hourly charge power, discharge power, and SOE of the battery, as well as hourly LPSP of the system, in this case, are depicted in Fig. 13. The optimum battery storage, in this case, is 6724.6kWh; therefore, the battery SOE fluctuation between maximum and minimum energy states (~5380 kWh and ~1345 kWh) is based on equation (12) and (13) as a guarantee of suitable performance of the batteries. As discussed earlier, there is a considerable heating load in both winter and autumn for Tokyo, resulting in a tricky situation this time of the year. It can be inferred from Fig. 13. That the battery SOE fluctuations are more frequent during these periods than the rest of the year. Also, the charge and discharge power of the battery, supporting the SOE fluctuations, are recurrent during winter and autumn. Consequently, loss of power supply is more liable in winter and autumn, as challenging periods of the year, than any other time. However, when reliability objective function (LPSP) weight increases, the LPSP drops to less than 1%, guaranteeing a reliable system.

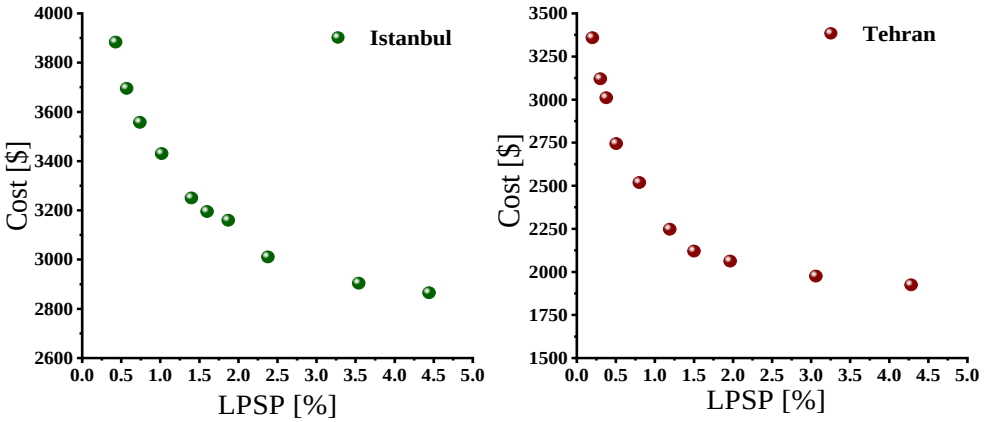


**Fig. 12.** Pareto frontiers for Istanbul and Tehran

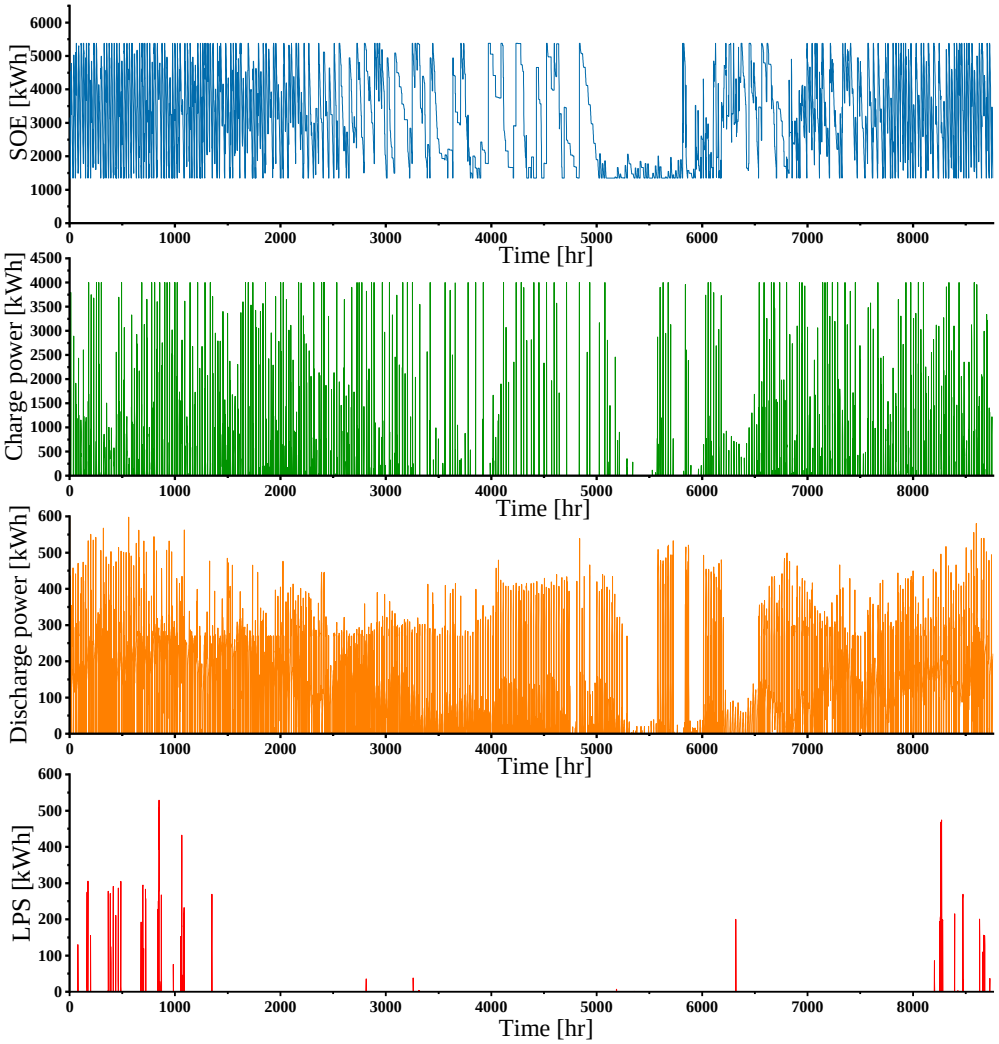


**Fig. 13.** Battery performance in one optimum result of Tokyo

## 4. Conclusion

In the present study, a stand-alone photovoltaic system is exhibited for a temporary residence in the ten most earthquake-prone cities worldwide: Tokyo, Jakarta, Manila, Los Angeles, Quito, Osaka, San Francisco, Lima, Tehran, Istanbul. The proposed PV system, including PV panel, HVAC system, and batteries, is optimized based on two objectives: LPSP and total cost of the system, using mixed-integer linear programming as a multi-objective optimization method. In this optimization, decision variables are specifications of PV panel (size and properties), HVAC system, and batteries.

Results have shown that the proposed photovoltaic system is beneficial for the intended purpose in the selected earthquake-prone cities, especially in regions with more significant solar radiation, such as Lima, Manila, Quito, and Los Angeles. Several options are attained for each city, employing a specific span for PV and storage system size in each city, resulting in a cost radius up to 4000$ in the most expensive options. Due to the electrical load demand and radiation amplitude during each period, there might be a challenging time for each city. This tricky period is mostly during winter and autumn when there is a significant heating load, and solar radiation is lower than the rest of the year. However, there are optimum solutions with LPSP lower than 1% for all cities, assuring a reliable energy system.

In summary, the following conclusions of this research can be implied as:

- The proposed stand-alone photovoltaic system for temporary residence is

undoubtedly a valuable option in earthquake-prone cities, resulting in almost no unmet electrical requirement during a year (less than 1%.)

- The photovoltaic system in cities enjoying a significant amount of solar radiation, such as Lima, Manila, Quito, Jakarta, and Los Angeles, cost about 2000$; however, in other cities with lower solar radiation or higher load demand, it increases up to 4000$.
- The optimum solutions of Lima, a subtropical desert South African city enjoying ample solar radiation, has the lowest cost and LPSP compared to others (up to 1800$.)
- On the other hand, the optimum solutions of Tokyo and Osaka, humid subtropical Japanese cities, have resulted in the biggest system size and consequently the highest cost of all (up to 4000$.)
- Backup energy systems such as a diesel engine or a wind turbine can be used in cities with higher load demand and lower solar radiation, including Tokyo, Osaka, Istanbul, Tehran, and San Francisco.

## References


[1] G. Merei, C. Berger, D.U. Sauer, Optimization of an off-grid hybrid PV–Wind–Diesel system with different battery technologies using genetic algorithm, Solar Energy 97 (2013) 460-473.

[2] K. Kaygusuz, Energy for sustainable development: A case of developing countries, Renewable and Sustainable Energy Reviews 16(2) (2012) 1116-1126.

[3] T. Khatib, A. Mohamed, K. Sopian, A review of photovoltaic systems size optimization techniques, Renewable and Sustainable Energy Reviews 22 (2013) 454-465.

[4] M. Fadaee, M. Radzi, Multi-objective optimization of a stand-alone hybrid renewable energy system by using evolutionary algorithms: A review, Renewable and sustainable energy reviews 16(5) (2012) 3364-3369.

[5] A. Ashouri, S.S. Fux, M.J. Benz, L. Guzzella, Optimal design and operation of building services using mixed-integer linear programming techniques, Energy 59 (2013) 365-376.

[6] D. Buoro, P. Pinamonti, M. Reini, Optimization of a Distributed Cogeneration System with solar district heating, Applied Energy 124 (2014) 298-308.

[7] C.O. Okoye, O. Taylan, D.K. Baker, Solar energy potentials in strategically located cities in Nigeria: Review, resource assessment and PV system design, Renewable and Sustainable Energy Reviews 55 (2016) 550-566.

[8] H.A. Kazem, T. Khatib, K. Sopian, Sizing of a standalone photovoltaic/battery system at minimum cost for remote housing electrification in Sohar, Oman, Energy and Buildings 61 (2013) 108-115.

[9] W.-S. Lee, Y.-T. Chen, Y. Kao, Optimal chiller loading by differential evolution algorithm for reducing energy consumption, Energy and Buildings 43(2-3) (2011) 599-604.

[10] Z.-f. Tan, L.-w. Ju, H.-h. Li, J.-y. Li, H.-j. Zhang, A two-stage scheduling optimization model and solution algorithm for wind power and energy storage system considering uncertainty and demand response, International Journal of Electrical Power & Energy Systems 63 (2014) 1057-1069.

[11] A.F.M. Nor, S. Salimin, M.N. Abdullah, M.N. Ismail, Application of artificial neural network in sizing a stand-alone photovoltaic system: a review, International Journal of Power Electronics and Drive Systems 11(1) (2020) 342.

[12] V. Modrák, R.S. Pandian, Operations Management Research and Cellular Manufacturing Systems: Innovative Methods and Approaches, Business Science Reference2012.

[13] N.D. Nordin, H.A. Rahman, A novel optimization method for designing stand alone photovoltaic system, Renewable Energy 89 (2016) 706-715.

[14] W. Shen, Optimally sizing of solar array and battery in a standalone photovoltaic system in Malaysia, Renewable energy 34(1) (2009) 348-352.

[15] T. Khatib, A. Mohamed, K. Sopian, M. Mahmoud, A new approach for optimal sizing of standalone photovoltaic systems, International Journal of Photoenergy 2012 (2012).

[16] R. Ayop, N.M. Isa, C.W. Tan, Components sizing of photovoltaic stand-alone system based on loss of power supply probability,

Renewable and Sustainable Energy Reviews 81 (2018) 2731-2743.
[17] M. Andam, J. El Alami, Y. Louartassi, Optimization of the Energy Lack and Surplus in a Stand-Alone Photovoltaic System, 2019 7th International Renewable and Sustainable Energy Conference (IRSEC), IEEE, 2019, pp. 1-6.
[18] L.A. Nguimdo, C. Kum, Optimization and Sizing of a Stand-Alone Photovoltaic System and Assessment of Random Load Fluctuation on Power Supply, Energy and Power Engineering 12(1) (2019) 28-43.
[19] A. Khalil, A. Asheibi, Optimal Sizing of Stand-alone PV System Using Grey Wolf optimization, 2019 International Conference on Electrical Engineering Research & Practice (ICEERP), IEEE, 2019, pp. 1-6.
[20] S. Semaoui, A.H. Arab, S. Bacha, B. Azoui, Optimal sizing of a stand-alone photovoltaic system with energy management in isolated areas, Energy Procedia 36 (2013) 358-368.
[21] A.B. Forough, R. Roshandel, Multi objective receding horizon optimization for optimal scheduling of hybrid renewable energy system, Energy and Buildings 150 (2017) 583-597.
[22] L. Hu, Y. Liu, D. Wang, J. Liu, Battery Capacity Reduction for Stand-Alone PV Air Conditioner by Using Curtailed Electricity to Store Chilled Water as a Backup, The International Symposium on Heating, Ventilation and Air Conditioning, Springer, 2019, pp. 609-617.
[23] M.S. Saleem, N. Abas, A.R. Kalair, S. Rauf, A. Haider, M.S. Tahir, M. Sagir, Design and optimization of hybrid solar-hydrogen generation system using TRNSYS, International Journal of Hydrogen Energy (2019).
[24] I. Dincer, M.A. Rosen, P. Ahmadi, Optimization of Energy Systems, John Wiley & Sons2017.
[25] C. Sexton, 10 cities most likely to be struck by an earthquake, 2017. https://www.earth.com/.
[26] 2015. https://www.worldometers.info/.
[27] 2021. https://worldpopulationreview.com/.
[28] M.C. Peel, B.L. Finlayson, T.A. McMahon, Updated world map of the Köppen-Geiger climate classification, Hydrology and earth system sciences 11(5) (2007) 1633-1644.
[29] S. Klein, W. Beckman, Loss-of-load probabilities for stand-alone photovoltaic systems, Solar Energy 39(6) (1987) 499-512.
[30] M.S.W.i.d.A.i. https://meteonorm.com/en/.
[31] TRNSYS: Transient System Simulation Tool. Available: http://www.trnsys.com/, 2016.
[32] R. Carapellucci, L. Giordano, Modeling and optimization of an energy generation island based on renewable technologies and hydrogen storage systems, International journal of hydrogen energy 37(3) (2012) 2081-2093.
[33] B. Huang, P. Hsu, M. Wu, P. Ho, System dynamic model and charging control of lead-acid battery for stand-alone solar PV system, Solar Energy 84(5) (2010) 822-830.
[34] S. Duryea, S. Islam, W. Lawrance, A battery management system for stand alone photovoltaic energy systems, Conference Record of the 1999 IEEE Industry Applications Conference. Thirty-Forth IAS Annual Meeting (Cat. No. 99CH36370), IEEE, 1999, pp. 2649-2654.
[35] A. Cherif, M. Jraidi, A. Dhouib, A battery ageing model used in stand alone PV systems, Journal of Power sources 112(1) (2002) 49-53.
[36] Y. Shin, W.Y. Koo, T.H. Kim, S. Jung, H. Kim, Capacity design and operation planning of a hybrid PV–wind–battery–diesel power generation system in the case of Deokjeok Island, Applied Thermal Engineering 89 (2015) 514-525.
[37] J. Li, W. Wei, J. Xiang, A simple sizing algorithm for stand-alone PV/wind/battery hybrid microgrids, Energies 5(12) (2012) 5307-5323.
[38] M. Hankins, Stand-alone solar electric systems: the earthscan expert handbook for planning, design and installation, Routledge2010.
[39] A. Roy, M.A. Kabir, Relative life cycle economic analysis of stand-alone solar PV and fossil fuel powered systems in Bangladesh with regard to load demand and market controlling factors, Renewable and Sustainable Energy Reviews 16(7) (2012) 4629-4637.
[40] C.O. Okoye, O. Solyalı, Optimal sizing of stand-alone photovoltaic systems in residential buildings, Energy 126 (2017) 573-584.

[41] A. Behzadi Forough, R. Roshandel, Multi objective optimization of solid oxide fuel cell stacks considering parameter effects: Fuel utilization and hydrogen cost, Journal of Renewable and Sustainable Energy 5(5) (2013) 053124.
[42] R. Roshandel, A. Behzadi Forough, Two strategies for multi-objective optimisation of solid oxide fuel cell stacks, International Journal of Sustainable Energy 33(4) (2014) 854-868.